Optics Letters

Nonsymmetric curved beams within a symmetric caustic skeleton

P. Frigerio Parenza,[1,2] D. Amaya,[1] Ó. Martínez-Matos,[3] and P. Vaveliuk[1,*]

[1]Centro de Investigaciones Ópticas (CICBA-CONICET-UNLP), Cno. Parque Centenario y 506, P.O. Box 3, 1897 Gonnet, Argentina
[2]Dpto. de Física, Facultad de Ciencias Exactas, Universidad Nacional de La Plata, P.O. Box 47, 1900 La Plata, Argentina
[3]Departamento de Óptica, Facultad de Ciencias Físicas, Universidad Complutense de Madrid, Av. Complutense s/n, 28040 Madrid, Spain
*Corresponding author: pablov@ciop.unlp.edu.ar

Received 17 May 2018; revised 24 July 2018; accepted 27 July 2018; posted 30 July 2018 (Doc. ID 331774); published 23 August 2018

Nonsymmetric curved beams having a symmetric caustic skeleton are presented. They arise from a finite jump in the symmetric spectral phase that breaks the symmetry of the beam intensity without altering its associated caustic curve. These nonsymmetric beams can be represented as a superposition of two caustic beams whose wave fields have well-defined even and odd symmetries with weight coefficients dependent on the phase jump. In this approach, the phase jump acts as a measure of the beam asymmetry degree that can be easily controlled in experiments. This scheme is a promising step towards optical cryptography and quantum optics applications.

OCIS codes: (140.3300) Laser beam shaping; (260.0260) Physical optics; (080.0080) Geometric optics; (070.2580) Paraxial wave optics; (350.5500) Propagation.

https://doi.org/10.1364/OL.43.004148

The main feature of curved beams, also called accelerating beams, is that their main intensity peak follows a curved spatial trajectory as the beam propagates. The most famous curved beam is the Airy beam [1], whose observation in 2007 [2] gave rise to a rapid growth in the theoretical and experimental investigation on curved beams. Nowadays this matter became one of the central topics in beam propagation and design and derived branches [3–7]. The curved trajectory is due to the intensity distribution that follows a spatial curve called caustic. It can be interpreted as the skeleton of the beam. Within an undulatory context, the caustic is the frontier between evanescent and propagating waves while, within a geometric approach, it is the envelope of families of rays forming a curve or a surface where light focuses [8–10]. There exists a direct relationship between the spectral phase of the curved beam and the geometry of its caustic skeleton: the symmetry and the power of the spectral phase define the type of caustic and the degree of caustic curvature, respectively [11]. In a bidimensional space, an antisymmetric spectral phase defines a fold caustic [8–10] whose skeleton and its spatial intensity pattern are both symmetric with respect to the Fourier transverse plane [11]. The greatest exponent is the Airy beam itself [1,2]. In return, a symmetric spectral phase defines a cusp caustic [8–10] whose skeleton and its spatial intensity pattern are both symmetric with respect to the propagation coordinate [11]. Representative examples are the Pearcey beam [12] and the symmetric Airy beam (SAB) arisen from the cubic phase symmetrization [13,14]. A signature of caustic beams is that the symmetry of the intensity pattern follows the symmetry of its caustic skeleton. This feature was observed for curved beams in (1 + 1)D [15–18], and for abruptly autofocusing beams [19,20] and tailoring beams [21] in (2 + 1)D. However, it will be demonstrated here that there are beams having a nonsymmetric intensity pattern on a symmetric caustic skeleton, breaking the above "golden rule." These peculiar beams arise from a jump of finite size in the symmetric spectral. This simple phase modification breaks the intensity symmetry while preserving the symmetry of the caustic skeleton. In this Letter, we develop an approach to characterize this class of curved beams whose asymmetry degree is fully controlled by the size of the spectral phase jump. We perform a numerical analysis showing its main propagation properties and suggest potential applications of such a peculiar phenomenon.

A (1 + 1)D curved beam propagating along the z-axis is described by the wave field $E = E_0\, u\, e^{i(2\pi/\lambda)z}$ with amplitude E_0, wavelength λ, and dimensionless wave function [13],

$$u(s,\xi) = \frac{e^{i\xi k^2}}{2\pi}\int_{-\infty}^{+\infty} A(K)e^{i\psi(K)}\; e^{-i\xi K^2/2}\; e^{iKs}\mathrm{d}K, \qquad (1)$$

that is expressed in terms of a K-symmetric real spectral amplitude $A(K)$ and a two times differentiable spectral phase $\psi(K)$. The other terms of the integrand of Eq. (1) are the paraxial propagator $e^{i\xi(k^2-K^2/2)}$ and the Fourier transform factor e^{iKs}. The dimensionless spatial frequency K and transverse coordinate $s = x/x_0$ are conjugate variables where x_0 is a transverse scale characterizing the beam size. The dimensionless propagation coordinate is $\xi = z\lambda/(2\pi x_0^2)$, and $k = (2\pi/\lambda)x_0$ is the normalized wavenumber. The curved beam has associated a caustic that can be viewed as the structural skeleton of the beam along which most of the light intensity is distributed. It is well known that $\psi(K)$ determines the form of this skeleton structure [11,18] through the first and second K-derivatives of the full phase of the integrand of Eq. (1) equated to zero,

$$\psi'(K) - \xi K + s = 0, \tag{2a}$$

$$\psi''(K) - \xi = 0. \tag{2b}$$

Equation (2a) evaluates the stationary points representing families of rays with linear trajectories in the $s\xi$ plane. The number of solutions of Eq. (2a) coincides with the number of rays intersecting at a given point (s, ξ). Equation (2b) indicates that the projection of the ray surface onto the $s\xi$-space gives rise to singularities identified as caustics. By eliminating K from Eqs. (2), one obtains the explicit equation for the caustic curve in the $s\xi$-space associated to the beam with the wave field given by Eq. (1). As a remark, there exist noncurved caustics parallel to the propagation axis that are associated to nondiffracting solutions of Helmholtz equations [22] that are not tied to the maximum of the intensity pattern. This type of caustic is not tackled by means of Eqs. (2).

Let us now introduce a finite gap of size β in half of the space K on a symmetric phase ψ. The modified phase is

$$\tilde{\psi}(K) = \begin{cases} \psi(K) & \text{if } K \geq 0 \\ \psi(K) + \beta & \text{if } K < 0, \end{cases} \tag{3}$$

giving rise to a new field $\tilde{u}(s, \xi)$ that only differs from $u(s, \xi)$ by the phase jump. The first and second derivatives of $\tilde{\psi}$ coincide with the first and second derivatives of ψ for all K except at $K = 0$, where a singularity exists. However, this is an avoidable singularity since the lateral limits of $\tilde{\psi}'(K)$ and $\tilde{\psi}''(K)$ result in the following:

$$\lim_{K\to 0^+} \tilde{\psi}'(K) = \lim_{K\to 0^-} \tilde{\psi}'(K) = \psi'(0). \tag{4a}$$

$$\lim_{K\to 0^+} \tilde{\psi}''(K) = \lim_{K\to 0^-} \tilde{\psi}''(K) = \psi''(0). \tag{4b}$$

Therefore, both derivative functions can be redefined at $K = 0$ to be continued functions with values $\tilde{\psi}'(0) = \psi'(0)$ and $\tilde{\psi}''(0) = \psi''(0)$. This renormalization ensures the equivalence between the first and second derivatives of $\tilde{\psi}$ and ψ. Hence, curved beams represented by wave fields u and $\tilde{u}$ possess identical caustic curves. Any finite jump β in the phase leaves invariant the caustic skeleton. Thereby, the antisymmetric Airy beam (ASAB), having an antisymmetric wave field [23], and the SAB, having a symmetric wave field, both differing by a π-jump in the cubic–symmetric spectral phase, possess the same cusp skeleton.

In Ref. [23], it was demonstrated that any beam emerged from a π-jump in the symmetric phase has an odd wave field with respect to s because it can be represented by a sine Fourier transform on that variable. Thereby, any pair of wave fields having even and odd s-symmetry, say u_e and u_o, possess jumps of size $\beta = 0$ and π in the phase [Eq. (3)]. They can be viewed as "pure parity states," and their s-parity is evident when the wave fields are expressed in terms of sine and cosine Fourier transforms [23],

$$u_e(s, \xi) = \frac{e^{i\xi k^2}}{\pi} \int_0^\infty A(K) e^{i\psi(K)}\ e^{-i\xi K^2/2}\ \cos(Ks) \mathrm{d}K, \tag{5a}$$

$$u_o(s, \xi) = \frac{ie^{i\xi k^2}}{\pi} \int_0^\infty A(K) e^{i\psi(K)}\ e^{-i\xi K^2/2}\ \sin(Ks) \mathrm{d}K, \tag{5b}$$

where ψ is the nonjump symmetric phase. The phases with $\beta \neq 0, \pi$ yield a wave field with no defined parity, i.e., a "mixed or nonpure parity field." This asymmetry in the wave field implies a mandatory asymmetry in the beam intensity pattern. In spite of this, the symmetric caustic skeleton corresponding to $\beta = 0, \pi$ holds for these nonsymmetric beams as it was proved through Eqs. (2)–(4). This breaks down the established idea for curved beams about how symmetric caustic skeletons necessarily lead to symmetric intensity patterns.

From the above, it is clear that the jump size β can be interpreted as a measure of parity degree of the wave field $\tilde{u}$, controlling the beam symmetry. Then, it is proper to express $\tilde{u}$ as a linear combination of linearly independent pure symmetric and antisymmetric fields given by Eqs. (5),

$$\tilde{u}(s, \xi) = C_e(\beta) u_e(s, \xi) + C_o(\beta) u_o(s, \xi), \tag{6}$$

where coefficients $C_e(\beta)$ and $C_o(\beta)$ give a measure of the weight that each pure field has on $\tilde{u}$. The aim is thus to find the explicit dependence of these coefficients on β and, thereby, to know the full dynamic of the nonsymmetric curved beams. This dependence is a key experimental matter since the parameter β can be fully controlled in a spatial light modulator (SLM). In order to derive C_e and C_o, we separate the integral [Eq. (1)] with spectral phase given by Eq. (3) into two parts, for $K < 0$ and for $K > 0$. Then, by expressing e^{iKs} in terms of sine and cosine and by accounting the even parity of $A(K)$ and $\psi(K)$, one finally obtains

$$\tilde{u}(s, \xi) = \left(\frac{1 + e^{i\beta}}{2}\right) u_e(s, \xi) + \left(\frac{1 - e^{i\beta}}{2}\right) u_o(s, \xi). \tag{7}$$

Equation (7) highlights the explicit β-dependence of the parity coefficients $C_e = (1 + e^{i\beta})/2$ and $C_o = (1 - e^{i\beta})/2$ and is the tool to analyze the dynamic of nonsymmetric curved beams. We restrict the analysis to the principal value $\beta \in [-\pi, \pi]$. It fulfills that $\beta = 0$ leads to $C_e = 1$ and $C_o = 0$ such that $\tilde{u} = u_e$, while for $\beta = \pm\pi$ leads to $C_e = 0$ and $C_o = 1$ being $\tilde{u} = u_o$, as expected. Any other β-value yields to a nonsymmetric wave field with nonzero coefficients C_e and C_o. The radiation intensity $\tilde{I}(s, \xi; \beta) = |\tilde{u}(s, \xi; \beta)|^2$ is constituted by three terms: the intensity of even and odd fields, I_e and I_o respectively, plus the interference or cross intensity, I_{cr}. Explicitly,

$$\begin{aligned} \tilde{I} &= I_e + I_o + I_{\mathrm{cr}} \\ &= |C_e|^2 |u_e|^2 + |C_o|^2 |u_o|^2 + 2\,\mathrm{Re}\{C_e C_o^* e^{i[\arg(u_e) - \arg(u_o)]}\} |u_e||u_o|, \end{aligned} \tag{8}$$

where $|C_e|^2 = \cos^2(\beta/2)$, $|C_o|^2 = \sin^2(\beta/2)$, and $C_e C_o^* = i(\sin\beta)/2$. Necessarily, $I_e, I_o \geq 0$, while I_{cr} is given by

$$I_{\mathrm{cr}}(\beta) = -\sin(\beta) \sin(\arg\ u_e - \arg\ u_o) |u_e||u_o|. \tag{9}$$

For $\beta = 0$, $I = I_e$, while for $\beta = \mp\pi$, $I = I_o$, as expected. Since I_e, I_o are even functions on both, s and β, the sum $I_e + I_o$ remains invariant for $s \to -s$ and $\beta \to -\beta$. In return, the behavior of the cross intensity is quite different. This is an odd function on s and on β, so that it necessarily yields a symmetry rupture of the beam intensity with respect to both parameters. The beam possessing the greatest asymmetry corresponds to $\beta = \pm\pi/2$ because $|I_{\mathrm{cr}}|$ reaches its maximum value. Only in this regime I_e and I_o are equi-weighted ($|C_e|^2 = |C_o|^2 = 1/2$). As an example, let us analyze the symmetry breaking on SAB and ASAB [13,23]. We numerically simulate I_{cr} as a function of (s, ξ). Figure 1 shows a density map of I_{cr} versus (s, ξ) for $\beta \in (0, \pi)$ [subfigure (a)] and for $\beta \in (-\pi, 0)$ [subfigure (b)]. Notice that one map is the s-inversion of the

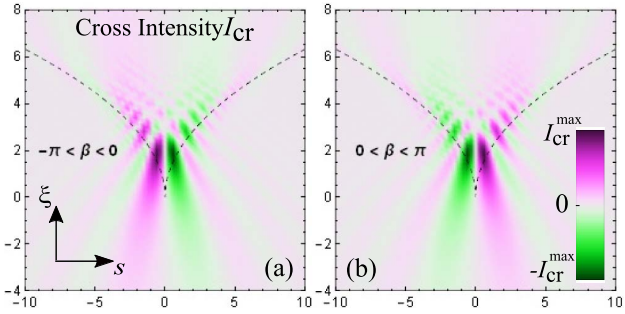

Fig. 1. Density plot of I_{cr} versus (s, ξ) for $\beta = \mp\pi/2$. The maps for β and $-\beta$ are inverted regarding $s = 0$. The dashed curve is the cusp caustic skeleton for SAB and ASAB.

other one, as expected by the antisymmetry of I_{cr} on β. It is evident that for $\beta \in (-\pi, 0)$, positive values of I_{cr} predominate for $s < 0$ and negative values dominate for $s > 0$, while the inverse happens for $\beta \in (0, \pi)$. This behavior determines where the total intensity will be enhanced and depleted, and therefore, it marks the dynamics of the asymmetry.

In order to deepen the analysis, we look to the behavior of the intensity distribution by varying the jump of the symmetric cubic phase, $\psi = |K|^3/3$. The amplitude is assumed to be $A = \exp(-aK^2)$ with $a = 0.08$. We evaluate the wave field through Eq. (1), where the phase was accounted by Eq. (3). In another way, we calculate u from the linear superposition of pure fields [Eq. (7)]. Thus, the intensity $I = uu*$ was evaluated from Eq. (1) and from Eq. (8), obtaining an identical result. This confirms the robustness of the wave field viewed as a superposition of symmetric and antisymmetric states. The numerical simulations are presented in Fig. 2. The sideway subfigures correspond to SAB and ASAB, whose phase jumps are 0 and $\mp\pi$, respectively. The inside subfigures depict nonsymmetric beams from nonpure parity fields. The first row of Fig. 2 emphasizes how the negative values of β enhance the total intensity for the main lobe at $s < 0$ while depleting the main lobe at $s > 0$. The maximum asymmetry is yielded at $\beta = -\pi/2$, where the I_{cr}-term has its maximum contribution. Besides, for $-\pi/2 < \beta < 0$, $|C_e|^2 > |C_o|^2$ such that the weight of I_e is greater than the weight of I_o, and the resultant beam will have more resemblance with the SAB. This is visualized for $\beta = -\pi/4$ in Fig. 2. In return, for $-\pi < \beta < -\pi/2$, $|C_o|^2 > |C_e|^2$ such that the resultant beam will have more resemblance with the ASAB (what is visualized for $\beta = -3\pi/4$). Looking for the second row where the intensities were obtained from positive phase jumps, a specular behavior of the intensity happens in relation to the ξ axis: the right-hand lobe is enhanced in detriment of the left-hand lobe in agreement with the antisymmetry of I_{cr}, shown in Fig. 1. In this manner, one can easily switch the intensity distribution with respect to the ξ axis by commuting the sign in the phase jump. In summary, Fig. 2 makes clear the feasibility of a succession of nonsymmetric curved beams within a symmetric caustic skeleton by only varying β. Notice that modulations in the spectral amplitude can yield interesting changes in the intensity pattern [24,25]. However, the asymmetry effect, in the approach studied here, is exclusively produced by the phase jump.

The predetermined manipulation of the phase jump β leads to a full control of the beam asymmetry through its intensity measured at any transverse plane, which could be useful in several applications. For instance, Fig. 3(a) shows the normalized intensity versus s for several values of $\beta > 0$ at the autofocusing plane. The huge on-axis intensity gap, ranged from the maximum value for the SAB to a null value for the ASAB, is apparent. Figure 3(b) shows the intensity profile at a further plane. A huge peak intensity gap between the right-hand side and left-hand side lobes is feasible, and they can be switched by $\beta \to -\beta$ (not shown in the figure) in a binary-like behavior. These results could be of interest since small changes in β give rise to huge changes in the intensity profile, which can be easily detected experimentally. We emphasize the potential usefulness in quantum optics and optical encryption. For the first, we refer to the generation of spatial qudits through a single SLM by using binary gratings [26]. This scheme presents a limit of the maximum intensity due to the low diffraction efficiency. Hence, the phase jump approach could be efficient due to the wide intensity range available. Moreover, it could avoid the use of a spatial filtering in the amplitude characterization of the quantum states since the intensity variations are fully controlled by the phase jump. For the second, the phase jump approach could be a powerful tool in optical information encryption

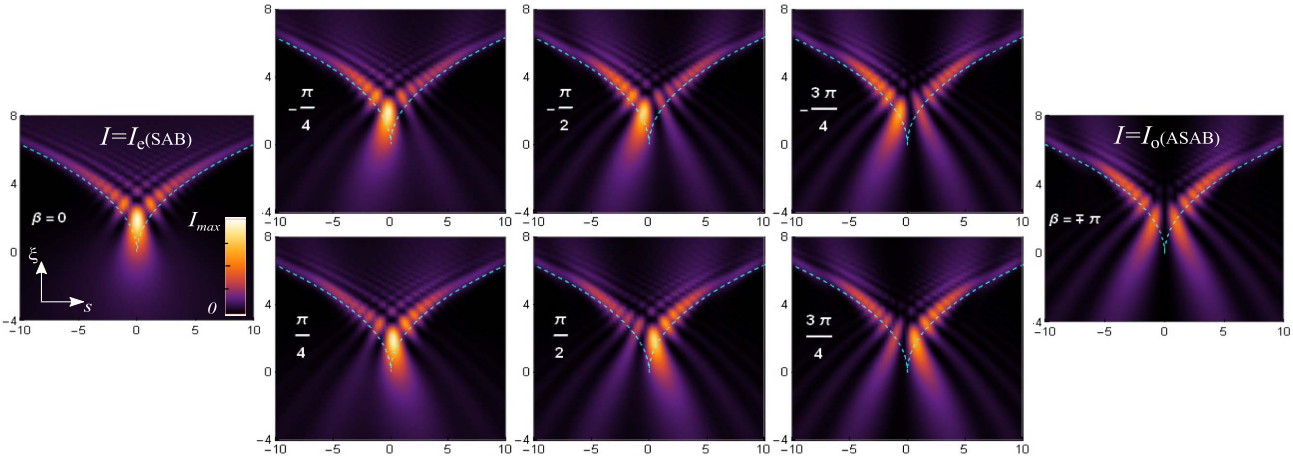

Fig. 2. Density plot of I versus (s, ξ) for nonsymmetric beams having a β-jump in the phase. The sideways subfigures represent the SAB and ASAB. The cusp caustic skeleton is represented by the dashed lines.

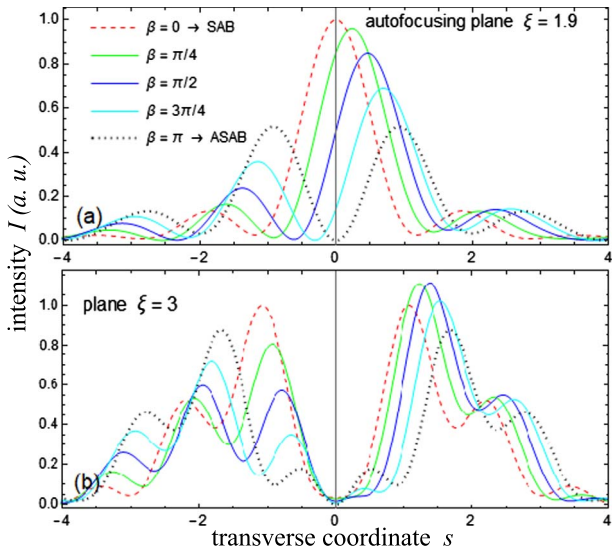

Fig. 3. I versus s for several values of $\beta > 0$. (a) profiles at autofocusing plane $\xi = 1.9$; (b) at $\xi = 3$. The intensity was normalized to the maximum intensity of the SAB at each plane.

in generating asymmetric keys [27] from the lobe intensity patterns controlled by the jump.

On the other hand, the above formalism, not limited to the symmetric cubic phase studied in this Letter, is valid for any beam arisen from any symmetric phase. For instance, the analysis could be performed on phases with powers less than two, as presented in Ref. [18], leading to peculiar families of nonsymmetric beams within unusual fold and cusp symmetric skeletons. Besides, the results presented here can be straightforwardly extended to two transverse dimensions due to the rectangular symmetry of all these beams.

Finally, one might ask what happens with a β-jump for an antisymmetric phase as it corresponds to the classical Airy beam. For such a case, the intensity is not more s-symmetric but ξ-symmetric [11,18]. As Eqs. (2)–(4) are valid no matter the phase symmetry, the caustic skeleton from an antisymmetric phase is also β-invariant. In the variable ξ, the field cannot be represented as a superposition of pure fields. Thereby, the parity degree concept is meaningless for beams arisen from a antisymmetric phase. Moreover, the ξ-symmetry of the beam is conserved regardless the β-jump, so that there is not breaking in the intensity symmetry with respect to that variable. It only produced an additional secondary interference pattern along the propagation axis that does not significantly alter the original beam.

In summary, a new class of curved beams having a nonsymmetric spatial intensity pattern within a symmetric caustic skeleton was presented. These beams arise from a finite jump in the symmetric spectral phase, and their dynamics are fully controlled by the parameter β. It was demonstrated that such a jump breaks down the spatial distribution of symmetry within the invariance of the caustic skeleton. These nonsymmetric beams exhibit peculiar features: they can be represented as a superposition of two caustic beams, one having a symmetric wave field and the other having an antisymmetric one. In this manner, the phase jump controls the parity degree of the beam and its dynamic just varying the β-value with a SLM. All these results can be directly extended to two transverse dimensions. The approach versatility along with its easy implementation opens the possibility to employ these beams in useful applications as optical encryption and quantum optics.

Funding. Consejo Nacional de Investigaciones Científicas y Técnicas (CONICET) (11220150100435); Agencia Nacional de Promoción Científica y Tecnológica, Argentina (3385), Ministerio de Economía y Competitividad (MINECO) (TEC2014-57394-P).

REFERENCES

1. G. A. Siviloglou and D. N. Christodoulides, Opt. Lett. **32**, 979 (2007).
2. G. A. Siviloglou, J. Broky, A. Dogariu, and D. N. Christodoulides, Phys. Rev. Lett. **99**, 213901 (2007).
3. Y. Hu, G. A. Siviloglou, P. Zhang, N. K. Efremidis, D. N. Christodoulides, and Z. Chen, in *Nonlinear Photonics and Novel Optical Phenomena*, Z. Chen and R. Morandotti, eds., Springer Series in Optical Sciences (Springer, 2012), Vol. **170**, pp. 1–46.
4. R. Schley, I. Kaminer, E. Greenfield, R. Bekenstein, Y. Lumer, and M. Segev, Nat. Commun. **5**, 5189 (2014).
5. T. Vettenburg, H. I. Dalgarno, J. Nylk, C. Coll-Lladó, D. E. Ferrier, T. Čižmár, F. J. Gunn-Moore, and K. Dholakia, Nat. Methods **11**, 541 (2014).
6. D. S. Simon, in *A Guided Tour of Light Beams* (Morgan & Claypool Publishers, 2016), pp. 6-1–6-5.
7. Y. Zhang, H. Zhong, M. R. Belić, and Y. Zhang, Appl. Sci. **7**, 341 (2017).
8. Yu. A. Kravtsov and Yu. I. Orlov, *Caustics, Catastrophes and Wave Fields*, 2nd ed. (Springer-Verlag, 1999).
9. M. V. Berry and C. Upstill, "Catastrophe optics: morphologies of caustics and their diffraction patterns," in *Progress in Optics IV*, E. Wolf, ed. (North Holland, 1890).
10. J. F. Nye, *Natural Focusing and Fine Structure of Light Caustics and Wave Dislocations* (Taylor & Francis, 1999).
11. P. Vaveliuk, A. Lencina, J. A. Rodrigo, and Ó. Martínez-Matos, Phys. Rev. A **92**, 033850 (2015).
12. J. D. Ring, J. Lindberg, A. Mourka, M. Mazilu, K. Dholakia, and M. R. Dennis, Opt. Express **20**, 18955 (2012).
13. P. Vaveliuk, A. Lencina, J. A. Rodrigo, and Ó. Martínez-Matos, Opt. Lett. **39**, 2370 (2014).
14. P. A. Quinto-Su and R. Jáuregui, Opt. Express **22**, 12283 (2014).
15. E. Greenfield, M. Segev, W. Walasik, and O. Raz, Phys. Rev. Lett. **106**, 213902 (2011).
16. L. Froehly, F. Courvoisier, A. Mathis, M. Jacquot, L. Furfaro, R. Giust, P. A. Lacourt, and J. M. Dudley, Opt. Express **19**, 16455 (2011).
17. Y. Hu, D. Bongiovanni, Z. Chen, and R. Morandotti, Phys. Rev. A **88**, 043809 (2013).
18. P. Vaveliuk, A. Lencina, and Ó. Martínez-Matos, Opt. Lett. **42**, 4008 (2017).
19. D. G. Papazoglou, N. K. Efremidis, D. N. Christodoulides, and S. Tzortzakis, Opt. Lett. **36**, 1842 (2011).
20. I. Chremmos, N. K. Efremidis, and D. N. Christodoulides, Opt. Lett. **36**, 1890 (2011).
21. Y. Wen, Y. Chen, Y. Zhang, H. Chen, and S. Yu, Phys. Rev. A **95**, 023825 (2017).
22. I. J. Macías, C. Rickenstorff-Parrao, O. J. Cabrera-Rosas, E. Espíndola-Ramos, S. A. Juárez-Reyes, P. Ortega-Vidals, G. Silva-Ortigoza, and C. T. Sosa-Sánchez, J. Opt. Soc. Am. A **35**, 267 (2018).
23. P. Vaveliuk, A. Lencina, J. A. Rodrigo, and O. Martínez-Matos, J. Opt. Soc. Am. A **32**, 443 (2015).
24. Y. Hu, D. Bongiovanni, Z. Chen, and R. Morandotti, Opt. Lett. **38**, 3387 (2013).
25. D. Bongiovanni, Y. Hu, B. Wetzel, R. A. Robles, G. Mendoza González, E. A. Marti-Panameño, Z. Chen, and R. Morandotti, Sci. Rep. **5**, 13197 (2015).
26. J. J. M. Varga, M. A. Solís-Prosser, L. Rebón, A. Arias, L. Neves, C. Iemmi, and S. Ledesma, J. Phys. Conf. Ser. **605**, 012035 (2015).
27. S. K. Rajput and N. K. Nishchal, J. Opt. Soc. Am. A **31**, 1233 (2014).